

1    **GEOSTATISTICS AS A TOOL TO IMPROVE THE**  
2    **NATURAL BACKGROUND LEVEL DEFINITION:**  
3    **AN APPLICATION IN GROUNDWATER**

4    *Dalla Libera Nico <sup>a)</sup>, Fabbri Paolo <sup>a(\*)</sup>, Mason Leonardo <sup>b</sup>, Piccinini Leonardo <sup>a</sup>, Pola Marco <sup>a</sup>*

5    <sup>a</sup> Department of Geosciences, University of Padova, Padova, Via G. Gradenigo, 6 – 35131, Italy

6    <sup>b</sup> ARPAV, Department of Venice, Mestre, Via Lissa, 6 – 30171, Italy

7    **ABSTRACT**

8    The UE BRIDGE project suggests calculating the Natural Background Level (NBL) as the 90th  
9    percentile of the distribution of the concentration data. This method is suited for large, spatially  
10   distributed datasets providing a regional value of NBL that could be higher than the Threshold  
11   Value (TV) set by every country. Therefore, the use of a unique regional NBL value, higher than  
12   TV, in dis-homogeneous areas from the hydro-geochemical perspective, could arise problems to  
13   distinguish between natural occurrences and anthropogenic contaminant sources. Hence, the goal of  
14   this study is to improve the NBL definition using the geostatistical approach, which allows  
15   reconstructing the contaminant spatial structure keeping in account geochemical and  
16   hydrogeological relationships. We retain this integrate mapping fundamental to evaluate the  
17   contaminant's distribution impact on the NBL value, giving indications to improve it. We decided  
18   to test this method on the Drainage Basin of Venice Lagoon (DBVL), an area in northeastern Italy  
19   notoriously affected by naturally occurring arsenic contamination, where the existing NBL is seven  
20   times higher than the TV. An available geochemical dataset collected by 50 piezometers was used

21 to reconstruct the spatial distribution of arsenic in the densely populated area of the DBVL. A  
22 cokriging approach was applied exploiting the geochemical relationships among As, Fe and  $\text{NH}_4^+$ .  
23 The obtained spatial predictions of arsenic concentrations was divided into three different zones: i)  
24 areas with an As concentration lower than the TV, ii) areas with an As concentration between the  
25 TV and the median of the values higher than the TV, and iii) areas with an As concentration higher  
26 than the median. Subsequently, following the BRIDGE suggestions, where enough samples were  
27 available, the 90th percentile for each zone was calculated to obtain a local NBL (LNBL).  
28 Differently from the original NBL, this local value gives more detailed water quality information  
29 accounting the hydrogeological and geochemical setting, and contaminant spatial variation. Hence,  
30 the definition of a LNBL could give more indications about the distinction between natural  
31 occurrence and anthropogenic contamination.

32 **Keywords:** Local Natural Background Level (LNBL), cokriging (COK), Arsenic and Drainage  
33 Basin to the Venice Lagoon (DBVL).

## 34 **1. INTRODUCTION**

35 The assessment of the groundwater quality and the impact of the human activities are important  
36 worldwide challenges. Actually, the assessment of groundwater body qualitative status is related to  
37 the definition of Natural Background levels (NBLs) and Threshold values (TVs). The first one is  
38 mainly linked to the system's hydro-geochemical settings, while the second is associated to the  
39 public health issue. The NBL definition is a well-known problem due to its complexity, its  
40 challenging estimation and the delicate consequences on the environmental protection. The NBL of  
41 an element or compound in groundwater represents the range of concentrations resulting from the  
42 interaction of different natural atmospheric, geological, chemical and biological process during the  
43 hydrological cycle, and it could be influenced by human activities (Edmunds and Shand, 2008;  
44 Hinsby et al., 2008a; Reimann and Garrett, 2005). By defining the NBL, it is necessary to know the  
45 extension and the hydro-geochemical characteristics of the groundwater body at risk, paying

46 attention to use data coming from the same aquifer body and collected far from anthropogenic  
47 sources of contamination, in order to obtain pristine water samples (Coetsier et al., 2009; Hinsby et  
48 al., 2008; Wendland et al., 2008). Many studies treat the problem of the NBL definition or the  
49 definition of new approaches to improve it (Coetsier et al., 2009; Ducci et al., 2016; Molinari et al.,  
50 2012; Preziosi et al., 2010; Rotiroti et al., 2013, 2015), since the NBL assumes importance  
51 discriminating the anthropogenic contamination from the natural occurrence. A first approach to  
52 estimate the NBL value into European groundwater bodies was suggested by Edmunds and Shand  
53 (2008), and it was based on a geochemical prospective rather than a statistical one. Actually, the  
54 European Community in accordance with the European “BRIDGE” project (Background cRiteria  
55 for the Identification of Groundwater thrEsholds) (Müller et al., 2006) suggests two main statistical  
56 method to estimate the NBL. The first approach, the “Component Separation” method (CP), is  
57 based on the distinguishable data distributions produced by the natural and anthropogenic sources  
58 that can be distinguished by a statistical analysis. In this approach, the observed concentration  
59 frequency distribution is fitted by the superimposition of two different distributions that represent  
60 the natural and the anthropogenic concentrations. Once estimate the distribution (shape and  
61 statistical parameters) of the natural component, the data following it will be used to estimate the  
62 NBL. On the other hand, the second method suggests a pre-selection of the data basing on some  
63 markers’ concentration that point an anthropogenic contamination out (e.g. nitrate, salinity, etc.).  
64 The basic idea of this method is that there is a correlation between the markers’ concentrations and  
65 the presence of an anthropogenic pressure. Thus, where the markers show concentration values over  
66 the pre-defined limits, the groundwater samples are excluded from the NBL estimation.  
67 Subsequently, for both methods, the NBL is estimated as the 90<sup>th</sup> or 97<sup>th</sup> percentile of the modified  
68 distribution of the concentration data (Coetsiers et al., 2009; Müller et al., 2006; Wendland et al.,  
69 2008b). These approaches give a unique NBL value for the entire area, which seems to be not  
70 capable to represent the local variation of the geochemical and environmental conditions. The  
71 definition of a unique NBL value for a large area, in fact, could make a considerable uncertainty

72 defining the contaminant's natural occurrence against an anthropogenic source. Considering both  
73 the importance of the health problem related to the contaminant natural occurrence and the  
74 complexity to define an exhaustive NBL value, this study aims to improve the NBL concept by  
75 using geostatistical methodology such as cokriging predictor (COK). This method, like other types  
76 of kriging, allows redefining the NBL as function of the spatial distribution of contaminant  
77 concentration. However, the COK keeps also in consideration the relationships among the target  
78 contaminant and other, geochemically related, dissolved species in groundwater. This methodology  
79 is applied on the case of the Drainage Basin of the Venice lagoon (DBVL) notoriously affected by  
80 both high natural and anthropic concentrations of arsenic. Furthermore, the Regional Agency for  
81 Environmental Protection and Prevention of Veneto (ARPAV) through the "A.Li.Na" project  
82 (ARPAV, 2014) estimated an arsenic NBL of 74  $\mu\text{g/L}$  that is seven times higher than the Threshold  
83 Value (TV=10  $\mu\text{g/L}$ ) defined by the annex III in the Commission Staff Working report of the EU's  
84 Groundwater Directive (GWD 2006/118/EC). However, the results of this project pointed out the  
85 importance of a detailed and local NBL accounting the complex and laterally variable geological  
86 and hydro-chemical settings. The results of our study could be useful to improve the definition of  
87 the NBL because it exploit the knowledge about the spatial structure and uncertainty of the  
88 naturally occurring contaminant into groundwater, giving a local detail that considers the  
89 environmental background. In addition, they could be used by the stakeholders to perform a more  
90 complete and explanatory plan for the environmental management.

## 91 **2. KNOWLEDGE ABOUT ARSENIC CONTAMINATION**

92 High arsenic concentrations in groundwater have been documented in several countries, such as  
93 Bangladesh, India (McArthur et al., 2001; Nickson et al., 1998, 2000), Vietnam (Fendorf et al.,  
94 2010), Hungary and the USA (Sorg et al., 2014; Welch et al., 2000). The natural occurrence of  
95 arsenic in these countries is often linked to the alluvial plain systems, but high arsenic  
96 concentrations can be found in volcanic environments or mining districts (e.g., Argentina, Chile,

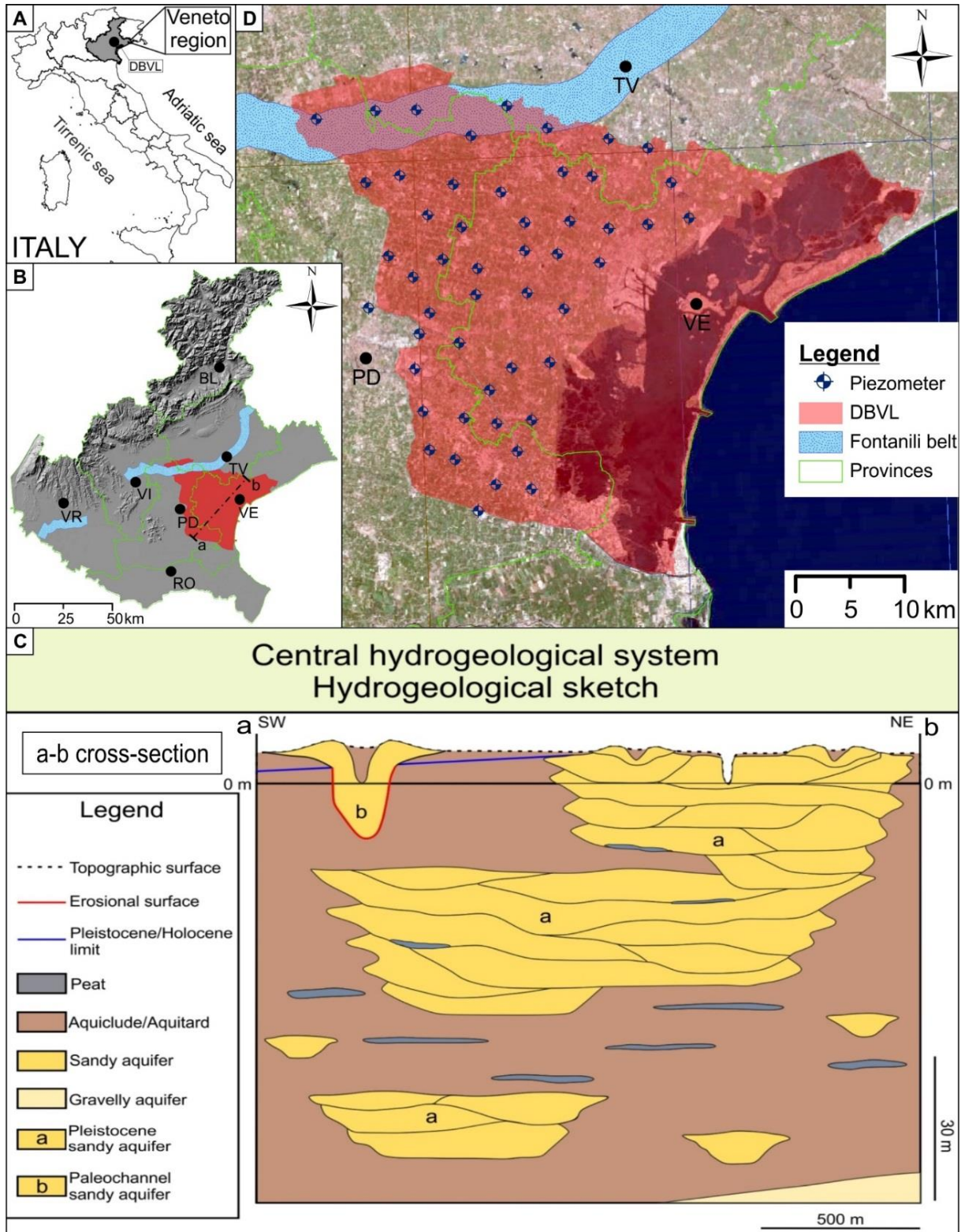
97 Brazil, Ethiopia, Greece and Italy) (Nordstrom, 2003; Rango et al., 2013). In Italy, high natural  
98 concentrations of arsenic in groundwater have been documented in volcanic aquifers of the central  
99 and southern Italy related to the uprising of geothermal fluids (Baiocchi et al., 2011; Ducci et al.,  
100 2016; Preziosi et al., 2010). Furthermore, in northern Italy, a high arsenic concentration can be  
101 found in the alluvial aquifers of the Po Plain (Molinari et al., 2013; Rotiroti and Fumagalli, 2013;  
102 Rotiroti et al., 2014; Zavatti et al., 1995) and the Venetian Plain (Carraro et al., 2013; Ungaro et al.,  
103 2008). Few materials (e.g., gold or sulfide mineral deposits, volcanogenic sources, alluvial  
104 sediments and organic matter) are currently recognized as significant sources of arsenic or drivers  
105 for its mobilization in groundwater. Nevertheless, the occurrence of arsenic in groundwater could  
106 be caused by anthropic activities, such as mineral extraction, industrial processes or fertilizer use.  
107 Arsenic is a metalloid that has three oxidation states nevertheless the most common forms in  
108 groundwater are the followings: the first is oxidized with an oxidation number (ON) equal to + 5,  
109 whereas the second is reduced with an ON equal to + 3. The reduced form appears to be more  
110 movable than the oxidized form in an aqueous medium, although both species have good mobility.  
111 The arsenic toxicity is due to its affinity to Phosphorus (P) that could be replaced by arsenic (As) in  
112 the metabolic processes of RNA and DNA synthesis. Arsenic is not widespread in the Earth's  
113 continental crust but is commonly concentrated in sulfide-bearing mineral deposits associated with  
114 Pyrite or Fe-hydroxides. Furthermore, many geothermal waters naturally exceed the TV of 10 µg/L.  
115 As determined in many studies, arsenic often is adsorbed onto Fe-Mn oxides or hydroxides, as well  
116 as into the organic matter (Baviskar et al., 2015; Carraro et al., 2015; McArthur et al., 2004, 2001,  
117 Molinari et al., 2015, 2013; Nickson et al., 2000; Rowland et al., 2007). Dissolution of these  
118 minerals in an acid-reducing environment causes the desorption processes that enable the release of  
119 As in an aqueous medium, exceeding its threshold value (McArthur et al., 2016; Smedley and  
120 Kinniburgh, 2002). Therefore, the organic matter could be a source of As, in addition to its role as a  
121 redox driver (Rotiroti et al., 2014). In particular, the release of As in groundwater is influenced by  
122 the variation of physical and chemical parameters, such as the Oxidation-Reduction Potential (ORP)

123 and pH (Smedley and Kinniburgh, 2002; Sorg et al., 2014), as well as the presence of elements and  
124 compounds that can promote its release (e.g.,  $\text{NO}_3^-$ ,  $\text{NH}_4^+$ ,  $\text{HCO}_3^-$ ,  $\text{SO}_4^{2-}$ ,  $\text{PO}_4^{3-}$ ) (Biswas et al., 2014).

### 125 **3. GEOLOGICAL AND HYDROGEOLOGICAL SETTINGS**

126 The study area is located in the middle-low Venetian Plain, including the Padua, Treviso and  
127 Venice provinces. The area covers approximately 2038 km<sup>2</sup> with a topographic gradient ranging  
128 from 0.6% to 0.1% near the Venice lagoon (Figure 1A, B). Two primary alluvial hydrogeological  
129 units occur in the Venetian plain: a large unconfined aquifer extending 15-20 km in the upper  
130 region of the plain from the foot of Prealps, and a multi-layered confined aquifer system in the  
131 lower region of the plain towards the Adriatic Sea. These two units correspond, respectively, to the  
132 upper and middle-lower plain environments. The plain spring's belt (named the "Fontanili" belt)  
133 shows the transition from the upper plain to the lower plain, where the water table is very shallow  
134 and locally intersects the topographic surface. From a geological perspective, the study area  
135 comprises gravelly and sandy alluvial deposits in the upper region near the "Fontanili" belt and  
136 silty-clayey deposits in the distal region (upper Pleistocene – Holocene) (Bondesan et al., 2004;  
137 Fontana et al., 2004, 2008; Mozzi et al., 2003). These fine sediments often contain peat layers  
138 formed in a floodplain environment, with a thickness of decimeters and a lateral extension of  
139 kilometers. The Drainage Basin to the Venice Lagoon (DBVL) extends to the lower plain  
140 environment, alternating silty layers with low permeability and sandy permeable layers, where the  
141 primary aquifers are located (Cambruzzi et al., 2009; Dal Prà et al., 1992; Fabbri and Piccinini,  
142 2013; Fabbri et al., 2011, 2013, 2016; Piccinini et al., 2015, 2016; Vorlicek et al., 2004) (Figure  
143 1C). Anyway, the subsoil structure of the DBVL is heterogeneous, due to the complex alluvial  
144 sedimentation processes that characterized the Brenta's alluvial plain (Trevisani and Fabbri, 2010)  
145 and surely influences the spatial distribution of As-bearing materials. This is important because  
146 Arsenic may be concentrated in sulfide-minerals, such as Pyrite ( $\text{FeS}_2$ ), or adsorbed onto oxides or  
147 hydroxides composing the fine portion of the alluvial sediments (Baviskar et al., 2015; Rowland et

148 al., 2007). Therefore, the peat layers play an important role in the arsenic release mechanism  
 149 because the degradation of the organic matter controls the aquifer's redox conditions and the thus  
 150 the dissolution of these As bearing minerals (Rotiroti et al., 2014).



151

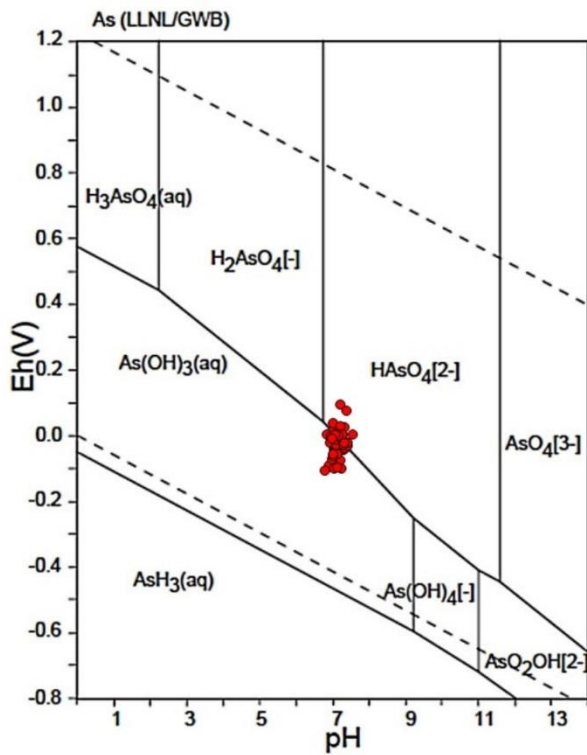
152 **Figure 1.** A) The location of the Veneto region in Italy; B) The location of the study area in the  
153 Veneto region, which covers the entire Brenta's Plain; C) A hydrogeological sketch of the low  
154 Brenta's Plain along the "a-b cross-section"; D) The piezometer locations in the DBVL. All of the  
155 piezometers are in the shallow aquifer, between 10 and 20 meter below ground level (BGL).

## 156 **4. MATERIALS AND METHODS**

### 157 **4.1.Dataset**

158 The data used in this work was obtained from the "A.Li.Na" project, which was developed to  
159 estimate the natural background levels (NBLs) of As, Fe, Mn and  $\text{NH}_4^+$  in the groundwater of the  
160 DBVL, according to the pre-selection method suggested by BRIDGE project. The hydro-  
161 geochemical sampling network (50 piezometers) was established with a variable spacing grid,  
162 covering all of the investigated area (Figure 1D). The sampled piezometers, used for NBL  
163 definition, are located far from the anthropogenic pollutant sources in order to obtain some pristine  
164 water samples. The piezometers tap the shallow aquifer at a depth of 10 – 20 meters below ground  
165 level (BGL). The hydro-geochemical parameters were collected during four seasonal surveys  
166 conducted from 2013 to 2014. The groundwater sampling was performed according to the standard  
167 protocols established by the Italian Environment Protection and Technical Services Agency (APAT,  
168 2006). In addition, the physical parameters (e.g., pH, ORP, electric conductivity, temperature and  
169 dissolved oxygen) were measured by a multi-parametric probe YSI mod. 556 MPS. The chemical  
170 parameters were estimated in the laboratory through standardized methods. Arsenic and Manganese  
171 were estimated by the UNI EN ISO 17294-2:2005 (revised by ISO 17294-2:2016) method, Iron by  
172 the APAT CNR IRSA 3160 Man 29 2003 method and Ammonium by the APAT CNR IRSA 4030  
173 A1 Man 29 2003 method (APAT, 2003). Furthermore, each sampling point was georeferenced in  
174 the Gauss-Boaga coordinate system (Roma 1940 datum, West zone). According to BRIDGE  
175 suggestions, the data were processed to estimate the average values from each available  
176 concentration time series, in order to create an average dataset that depicts the average system

177 behavior. Therefore, an average dataset was determined, depicting. Afterwards, the concentration  
 178 values below the limit of quantification (i.e.,  $\text{As} < 1 \mu\text{g/L}$ ) were changed to make the entire  
 179 “A.Li.Na” dataset suitable for mapping purposes. In such a case, the As concentrations below this  
 180 limit were set equal to  $0.5 \mu\text{g/L}$ . The DBVL shows high concentrations of arsenic in reducing  
 181 environments and often in association with rich organic matter reservoirs (Carraro et al., 2015;  
 182 Molinari et al., 2015; Rotiroti et al., 2014), according with the geological genesis of the area.  
 183 Looking at the Figure 2, the major part of the arsenic data show an ORP values from 0 mV to -150  
 184 mV and a pH between 7 and 8 according with the releasing as reduced forms.



185  
 186 **Figure 2.** A Pourbaix diagram of Arsenic species built under the conditions of  $T = 298.15 \text{ [}^\circ\text{K]}$  and  
 187  $P = 10^5 \text{ [Pa]}$ . The red dots represent the experimental data used for this study. The majority of the  
 188 sample data falls into the arsenic reduced species stability field (Takeno, 2005).

## 189 4.2. Geostatistical methods

190 The arsenic concentration in groundwater is linked to complex hydro-geochemical processes not yet  
191 well understood, hence its distribution in groundwater can be more usefully approached by  
192 geostatistical methods than by deterministic ones (e.g., Inverse Distance Weighting and Natural  
193 Neighbors). The geostatistical kriging predictor is based on a mixed model [1]:

$$\hat{Z}(\mathbf{u}_i) = R(\mathbf{u}_i) + m(\mathbf{u}_i) \quad [1]$$

194 where the predicted concentration  $\hat{Z}(\mathbf{u}_i)$ , at location  $\mathbf{u}_i$ , is composed of a residual component  $R(\mathbf{u}_i)$   
195 plus the mean  $m(\mathbf{u}_i)$ , representing, respectively, the stochastic component and the deterministic  
196 component of the predicted geostatistical concentration. Moreover, the kriging method needs to  
197 assume the stationary condition, considering the spatial correlation of the variable  $Z$  independent of  
198 their spatial position ( $\mathbf{u}_i$ ) but dependent only on the separation distance ( $h$ ) (Bivand et al., 2008;  
199 Isaak and Srivastava, 1989; Posa and De Iaco, 2009). Because the kriging predictor was built  
200 according to Equation [1], the problem is to define the mean  $m$  dependent on the position ( $\mathbf{u}_i$ ).  
201 Depending on the mean characteristics, three types of predictors can be considered as follows: i)  
202 Simple (co)kriging ( $m(\mathbf{u}_i)=m$ , the mean is known and constant), ii) Ordinary (co)kriging ( $m(\mathbf{u}_i)=m$ ,  
203 the mean is unknown but constant), and iii) Universal (co)kriging ( $m(\mathbf{u}_i)$ , the mean is not constant  
204 but defined by a spatial function). In the context of this study, the more acceptable condition was a  
205 mean that was constant within a moving search neighborhood but unknown, and thus, the selected  
206 prediction was an ordinary kriging approximation of  $\hat{Z}(\mathbf{u}_o)$ .

$$\hat{Z}(\mathbf{u}_o) = \sum_{i=1}^n \omega(\mathbf{u}_i) Z(\mathbf{u}_i) \quad [2]$$

207 If auxiliary variables correlated to the primary variable are available, a cokriging approach can be  
208 considered. Theoretically, it gives a prediction enhancement respect to ordinary kriging application.  
209 Cokriging is based on the same principles of kriging but also uses correlated auxiliary variables (in  
210 our case Fe and  $\text{NH}_4^+$ ) to predict the primary variable (in our case As).

$$\hat{Z}(\mathbf{u}_o) = \sum_{i=1}^n \omega(\mathbf{u}_i) Z(\mathbf{u}_i) + \sum_{j=1}^n \tau(\mathbf{u}_j) V(\mathbf{u}_j) \quad [3].$$

211 As evidenced in Equation [3], the cokriging predictor uses a weighted linear combination of the  
 212 principal variable  $Z(\mathbf{u}_i)$  and of the auxiliary variables  $V(\mathbf{u}_j)$  in the different position  $(\mathbf{u}_i)$  and  $(\mathbf{u}_j)$ . In  
 213 this manner, improving the principal variable prediction is possible. Using the matrix notation the  
 214 cokriging system is written as

$$\mathbf{K}_{CK} \mathbf{L}_{CK}(\mathbf{u}) = \mathbf{k}_{CK} \quad [4].$$

215 Where  $\mathbf{K}_{CK}$  is the  $n(\mathbf{u}) \times n(\mathbf{u})$  matrix of data covariances,  $\mathbf{L}_{CK}(\mathbf{u})$  is the vector of the weights  $\omega(\mathbf{u}_i)$   
 216 and  $\tau(\mathbf{u}_j)$ ,  $\mathbf{k}_{CK}$  represents the vector of data-to-unknown covariances. Basing on the [4], the  
 217 cokriging weights required by the COK estimator [3] are obtained by multiplying the inverse of the  
 218 data covariance matrix by the vector of data-to-unknown covariances:

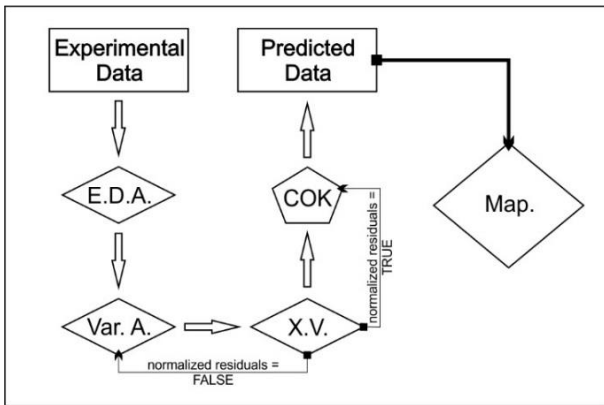
$$\mathbf{L}_{CK}(\mathbf{u}) = \mathbf{K}_{CK}^{-1} \mathbf{k}_{CK} \quad [5].$$

219 Furthermore, to satisfy the stationary and unbiased conditions, the estimated weights from [5] have  
 220 to undergo the following constrains:

$$\begin{cases} \sum_{i=1}^n \omega_i(\mathbf{u}) = 1, \\ \sum_{j=1}^n \tau_j(\mathbf{u}) = 0. \end{cases} \quad [6].$$

221 As reported in literature, cokriging method work better when the primary variable is less sampled  
 222 respect to the auxiliary one. Furthermore, one could also use it when main and auxiliary variable are  
 223 sampled in the same location (collocated cokriging) even if it gives lower prediction advantage than  
 224 the classical application. Nevertheless, in our study we consider the collocated cokriging method  
 225 because it produces a reduction on prediction error around 10% respect to OK. The geostatistical  
 226 analysis was conducted in the R environment (R Core Team, 2015), in particular with the gstat  
 227 package (Pebesma, 2004). The logical process (Figure 3) to estimate the arsenic spatial distribution

228 was composed of four primary steps: Exploratory Data Analysis, Variographic Analysis, Cross-  
229 validation, Ordinary cokriging.



230  
231 **Figure 3.** The flow chart of the classical logical process implemented in the geostatistical analysis.  
232 E.D.A = Exploratory Data Analysis, Var.A. = Variographic Analysis, X.V. = Cross-Validation,  
233 COK = Ordinary cokriging, Map. = Mapping the predicted principal variable.

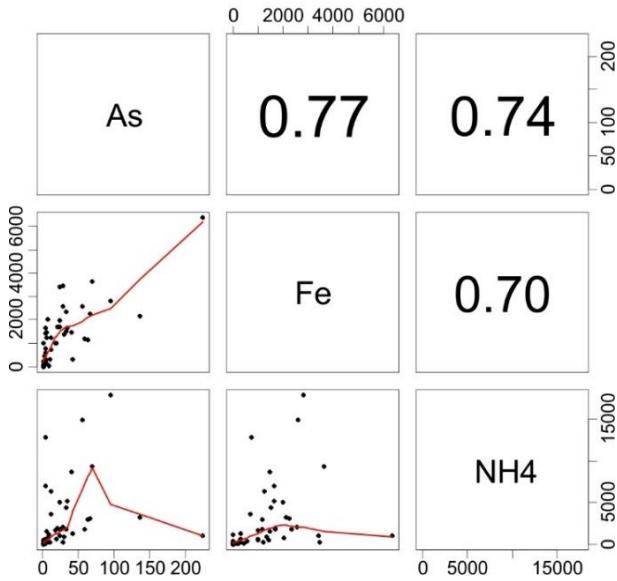
234

## 235 5. RESULTS AND DISCUSSION

### 236 5.1. Geostatistical analysis

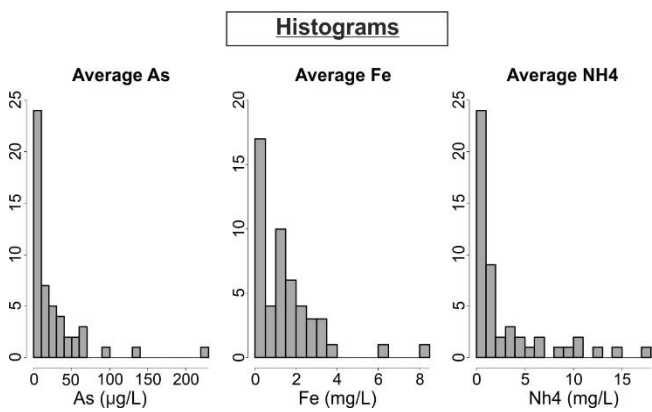
237 According to the goal of this study, the average dataset was considered. Initially, a study of the  
238 correlations between arsenic and other related chemical components (i.e., iron and ammonium) was  
239 performed. The robust correlation among As and other parameters indicated that the cokriging  
240 (COK) approach might be appropriate. To evaluate the correlation, we used a Spearman's  
241 correlation test and scatterplots. The Spearman's correlation test was selected because the  
242 experimental data do not have a normal distribution and the relation among the variables is not  
243 linear, so the Pearson's coefficient could be less exhaustive (Isaak and Srivastava, 1989). In that  
244 case, the Spearman's test, basing on ranks correlation, allows evaluating the strength of the  
245 correlation among the variables even if it is not linear. In addition, the scatterplot graphically  
246 explores linear correlations. The relationships among As, Fe and  $\text{NH}_4^+$  are illustrated in Figure 4 in  
247 which the scatterplots show the poor linear correlation between two variables emphasized by the  
248 local regression function LOESS (red line) and the numerical coefficients represent the Spearman's  
249  $\rho$ . The juxtaposition of these elements allow showing the poor relevance of the linear correlation on  
250 our data. The Spearman's  $\rho$  is greater than 0.5 and statistically meaningful (p-value < 5%  
251 significance level). Based on these relationships, we decided to use Fe and  $\text{NH}_4^+$  as the auxiliary  
252 variables in the COK prediction process of As. Subsequently, histograms, scatterplots explored the  
253 statistical structure of the raw data. In this manner, estimating the statistical parameters of the data  
254 (i.e., means, standard deviation, variance, skewness, etc.) was possible. Arsenic, iron and  
255 ammonium data followed a lognormal distribution with positive skewness coefficients (3.13, 2.20,  
256 1.87, respectively; Figure 5). The raw data were transformed to a normal score in order to perform a  
257 COK prediction with lower error as possible. Furthermore, the normal score transformation allows  
258 an easier back-transformation of the processed data, giving lower error respect to the use of log-  
259 transformation.

**Correlation Scatterplot Matrix (Spearman's rho)**



260

261 **Figure 4.** A correlation scatterplot matrix based on Spearman's method, providing the  $\rho$   
 262 coefficients for the pairs As-Fe, As-NH<sub>4</sub><sup>+</sup> and Fe-NH<sub>4</sub><sup>+</sup>. In the lower part of the matrix, the  
 263 scatterplot related to the variable pairs are shown. They represent the poor linear correlation  
 264 emphasized by the red line that represents the local regression function LOESS (Cleveland, 1979).  
 265 The correlation coefficients  $\rho$  are shown in the upper part of the matrix. The used dataset is the  
 266 average of the four surveys and the Spearman's correlation test was conducted with the  
 267 experimental concentration variables.



268

269

270 **Figure 5.** The three histograms represent the distributions of the average data of As, Fe and NH<sub>4</sub><sup>+</sup>,  
 271 respectively.

272 The second step of the geostatistical process was the Variographic Analysis of the transformed data.  
 273 The variogram  $\gamma(h)$  describes how spatial continuity changes with the distance (h) and the direction.  
 274 In addition, the cokriging approach requires the variogram and the cross-variogram analyses. An  
 275 analysis of the surface variograms in Figure 6A did not reveal any anisotropy in the continuity  
 276 structures of the studied variables. Considering this, only omnidirectional variograms and cross-  
 277 variograms were considered (Figure 6B). A Linear Model of Co-regionalization (LMC) fits a  
 278 theoretical variogram model with both experimental variograms and cross-variograms. The LMC  
 279 provides authorized theoretical models of variograms and cross-variograms of two or more  
 280 variables so that the variance of any possible linear combination of these variables is always  
 281 positive (Isaak and Srivastava, 1989). The resulting theoretical variograms (Figure 6) were used  
 282 during the cokriging prediction. The variogram model used in this study was spherical both for  
 283 auto- and cross-variograms:

$$\gamma(h) = \begin{cases} nu + c; & |h| > a \\ nu + c \left[ \frac{3|h|}{2a} - \frac{1}{2} \left( \frac{|h|}{a} \right)^3 \right]; & |h| \leq a \end{cases} \quad [7].$$

284 where nu is the nugget effect, c represents the partial sill and a represents the range. The variogram  
 285 models referred to As, Fe and  $\text{NH}_4^+$ , and the three cross-variogram models of As-Fe, As- $\text{NH}_4^+$  and  
 286 Fe- $\text{NH}_4^+$  are visible in Table 1.

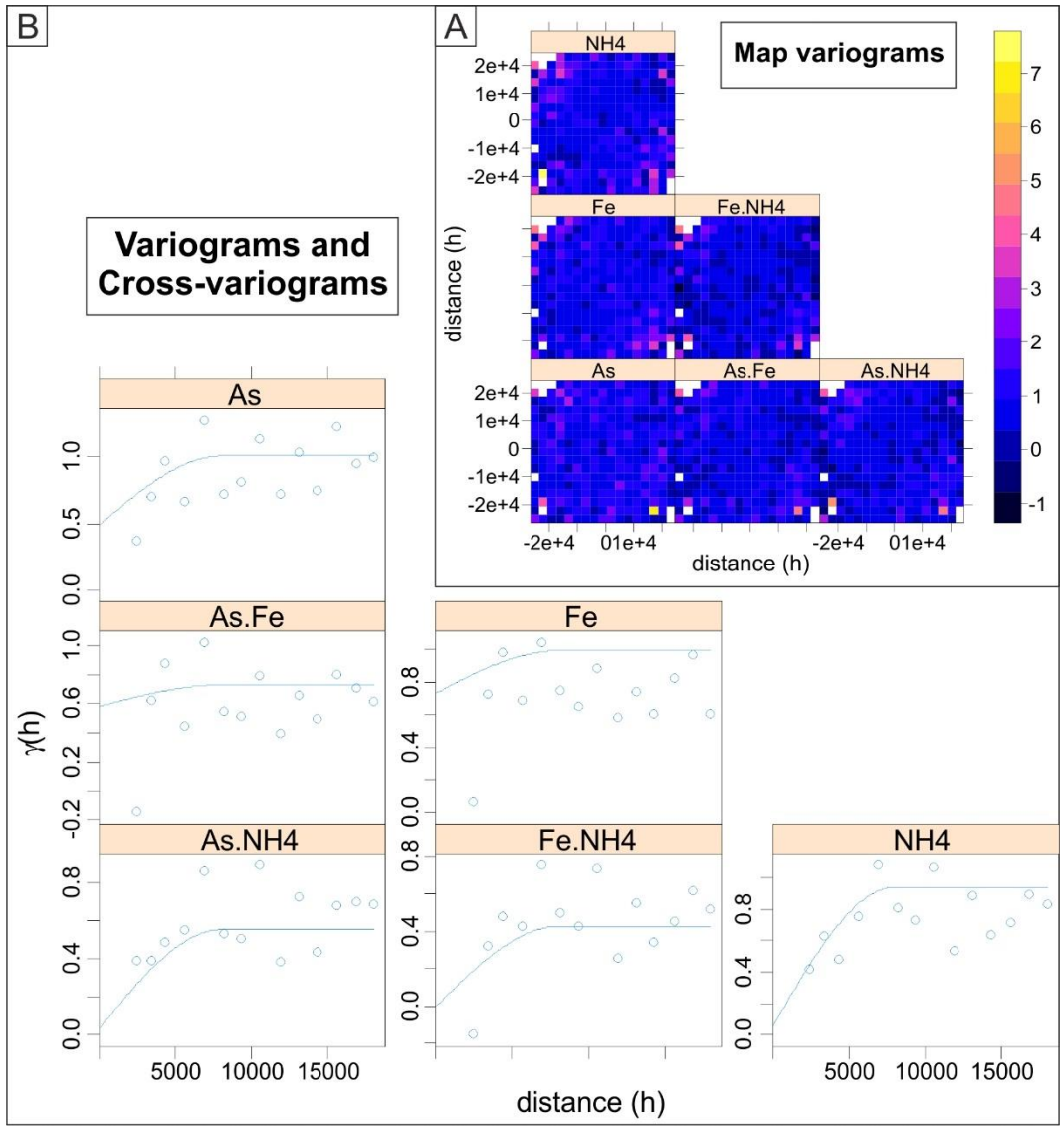
287

288 **Table 1. The variogram and cross-variogram models used to predict the arsenic spatial**  
 289 **distribution.**

Variogram model	Parameter
$\gamma(h) = \begin{cases} 0.486 + 0.523; &  h  > 8000 \\ 0.486 + 0.523 \left[ \frac{3 h }{2 \cdot 8000} - \frac{1}{2} \left( \frac{ h }{8000} \right)^3 \right]; &  h  \leq 8000 \end{cases}$	[As]
$\gamma(h) = \begin{cases} 0.730 + 0.260; &  h  > 8000 \\ 0.730 + 0.260 \left[ \frac{3 h }{2 \cdot 8000} - \frac{1}{2} \left( \frac{ h }{8000} \right)^3 \right]; &  h  \leq 8000 \end{cases}$	[Fe]

$\gamma(h) = \begin{cases} 0.055 + 0.884; &  h  > 8000 \\ 0.055 + 0.884 \left[ \frac{3}{2} \frac{ h }{8000} - \frac{1}{2} \left( \frac{ h }{8000} \right)^3 \right]; &  h  \leq 8000 \end{cases}$	[NH <sub>4</sub> <sup>+</sup> ]
$\gamma(h) = \begin{cases} 0.581 + 0.148; &  h  > 8000 \\ 0.581 + 0.148 \left[ \frac{3}{2} \frac{ h }{8000} - \frac{1}{2} \left( \frac{ h }{8000} \right)^3 \right]; &  h  \leq 8000 \end{cases}$	[As-Fe]
$\gamma(h) = \begin{cases} 0.034 + 0.521; &  h  > 8000 \\ 0.034 + 0.521 \left[ \frac{3}{2} \frac{ h }{8000} - \frac{1}{2} \left( \frac{ h }{8000} \right)^3 \right]; &  h  \leq 8000 \end{cases}$	[As-NH <sub>4</sub> <sup>+</sup> ]
$\gamma(h) = \begin{cases} -0.004 + 0.429; &  h  > 8000 \\ -0.004 + 0.429 \left[ \frac{3}{2} \frac{ h }{8000} - \frac{1}{2} \left( \frac{ h }{8000} \right)^3 \right]; &  h  \leq 8000 \end{cases}$	[Fe-NH <sub>4</sub> <sup>+</sup> ]

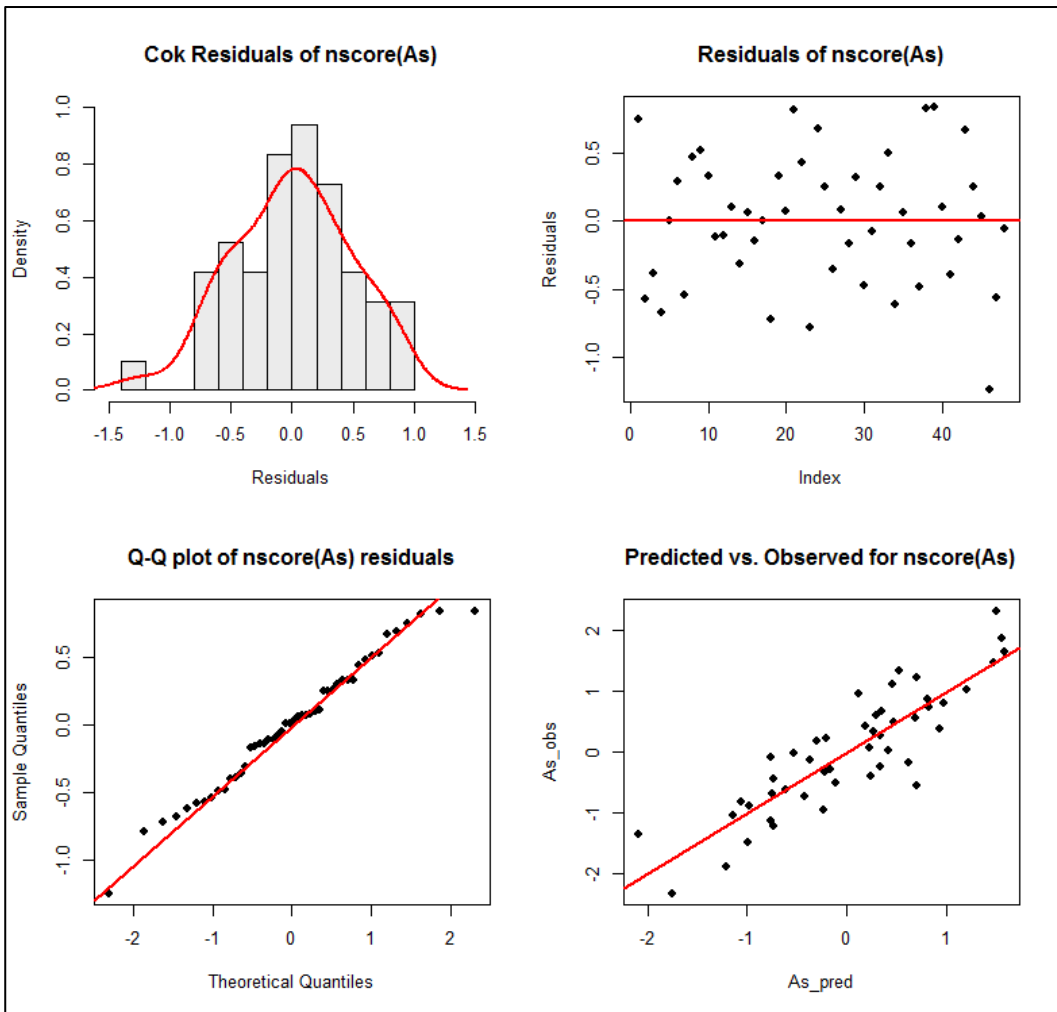
290



291

292 **Figure 6.** A) The surface variograms and cross-variograms. The surface variograms are shown in  
293 the first column. B) The omnidirectional variogram and cross-variograms. The variograms are on  
294 the diagonal, and the associated cross-variograms (referred to the average values of surveys) are  
295 below the diagonal.

296 Following the above variogram analysis, a cross-validation procedure was applied. The cross-  
297 validation tests the ability of the model to reproduce the spatial continuity structure by the  
298 prediction of the used dataset. The cross-validation, applied on our data, gives a mean estimation  
299 error equal to 0.001  $\mu\text{g/L}$ , confirming the good prediction given by the chosen variogram model  
300 (Isaak and Srivastava, 1989). Looking the Figure 7, it is evident the normality of the estimation  
301 errors and the good reproduction of the experimental data, highlighting the model's goodness.  
302 Furthermore, in our case, the cross-validation resulted in an acceptable normalized root mean  
303 square error (nRMSE) equal to 13.3%, which is around 10% lower than the nRMSE obtained by the  
304 ordinary kriging prediction on the same data. A similar nRMSE is likely linked to the presence of  
305 punctual high values of arsenic (hot spots), influencing the prediction process. Generally, the  
306 problems linked to the hot spots are common in environmental datasets.



307

308 **Figure 7:** Graphical representation of the arsenic residuals coming from the cross-validation  
 309 process by assessing the goodness of the chosen spatial model. Moving from the upper left corner  
 310 toward the lower right one, there are the probability density function of residuals, the distribution  
 311 around the zero value, the QQ-norm plot and the scatterplot observed As vs. predicted As. In the  
 312 last diagram, the red line represents the linear trend line (correlation coeff. = 0.67)

313 **5.2.Arsenic distribution**

314 Following the previous geostatistical analysis, an ordinary cokriging predictor was applied. The  
315 prediction process allowed mapping the arsenic distribution on the shallow groundwater of the  
316 DBVL (Figure 8). By improving the NBL concept and getting a more detailed value, we decided to  
317 consider the TV and the median (M) of the original dataset as thresholds to reclassify the  
318 distribution map. The reclassification process is necessary to identify the data that have similar  
319 arsenic values and then estimate some Local NBL following the 90<sup>th</sup> percentile method. In our case,  
320 the median was chosen because the “A.Li.Na” NBL value is several times higher than the TV and it  
321 seems adequate as intermediate threshold, separating the 50% of the data. However, the choice of  
322 the intermediate threshold is linked to both the dataset structure and the gap between the existing  
323 NBL and TV. In this way, we are able to define some sub-area in which estimate, effectively, some  
324 local NBL (LNBL) values (Table 2). A unique value of NBL does not seem to be realistic in  
325 regional environments with a large variation of concentrations.

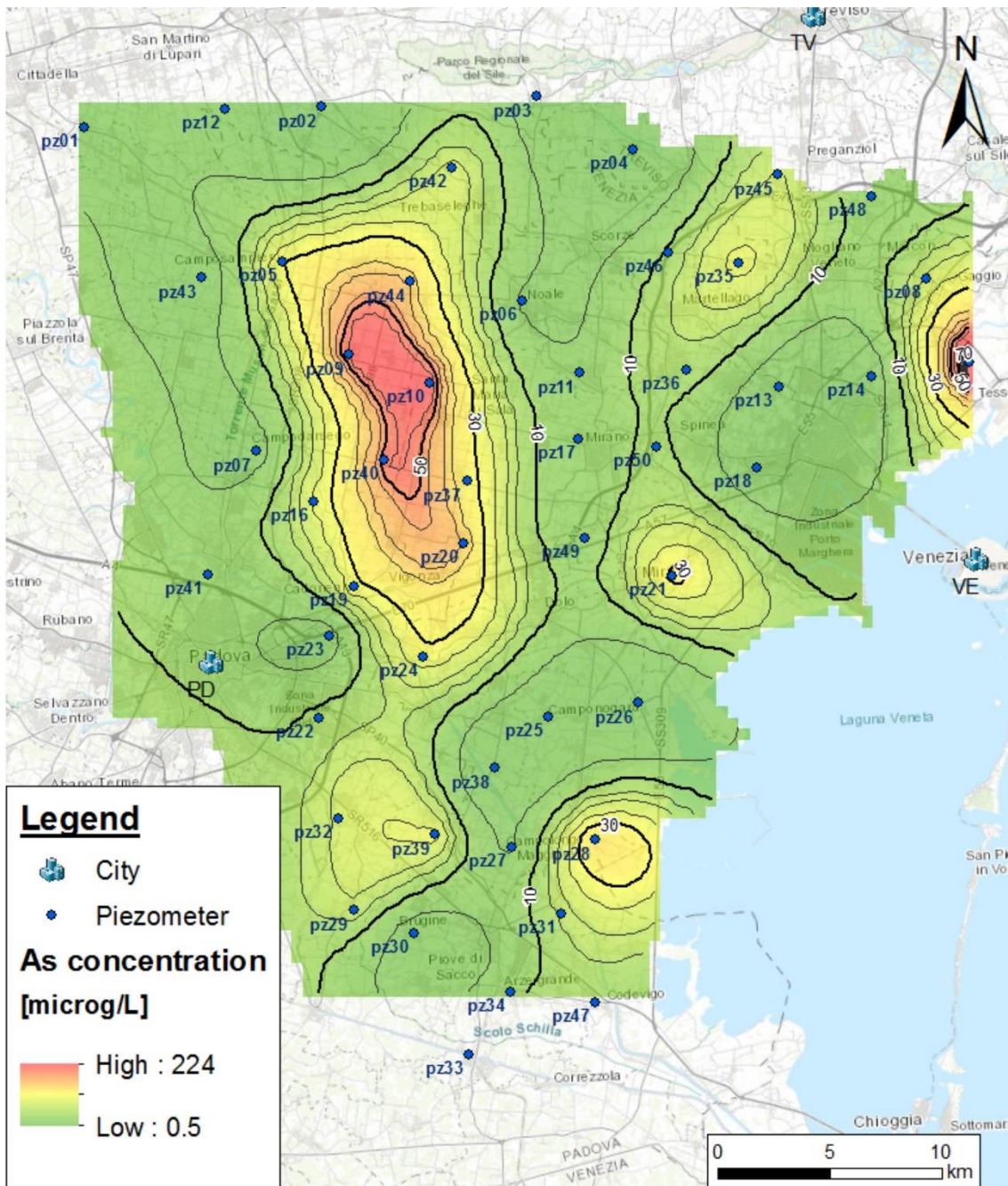
326 **Table 2. Arsenic concentration classes used to evaluate the LNBLs.**

1 <sup>st</sup>	As ≤ 10 µg/L (TV)	Lower (LNBL <sub>L</sub> )
2 <sup>nd</sup>	10 < As ≤ 31.4 µg/L (M)	Intermediate (LNBL <sub>I</sub> )
3 <sup>rd</sup>	As > 31.4 µg/L	Higher (LNBL <sub>H</sub> )

327

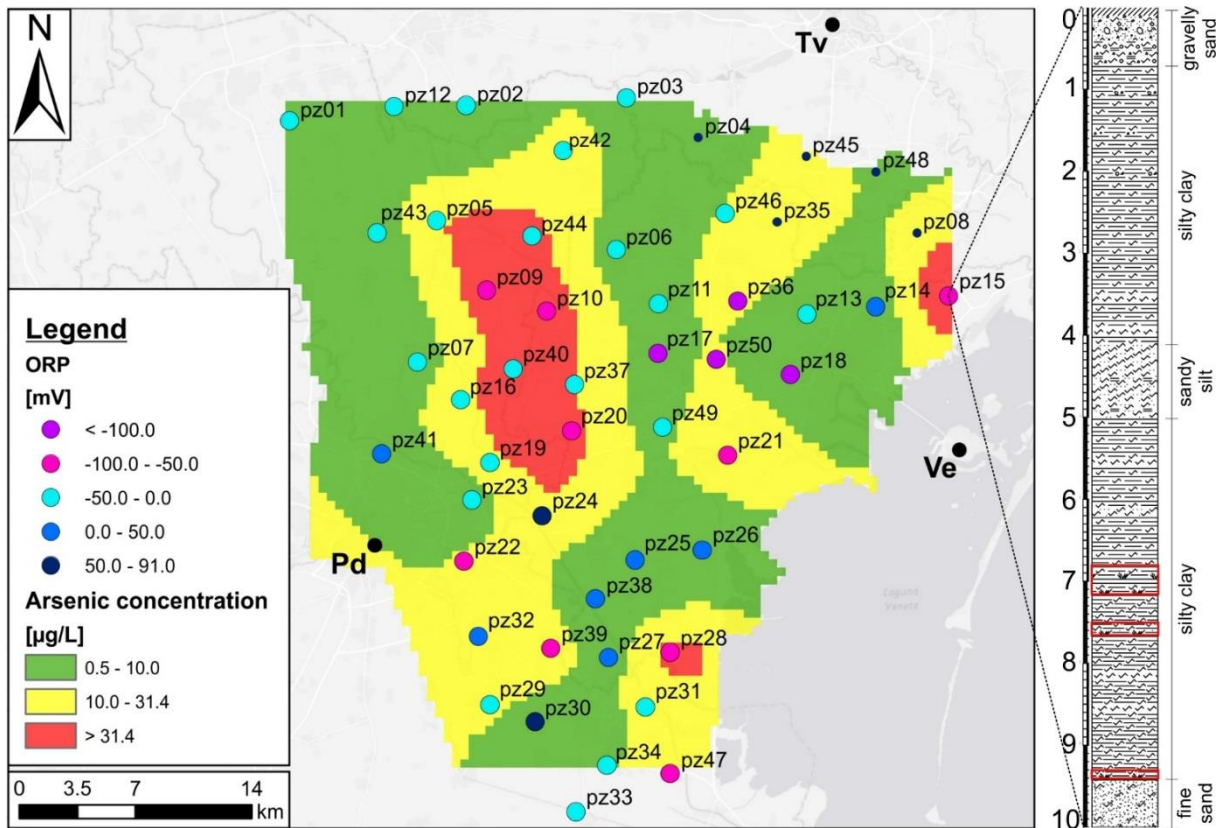
328 According to the above-described thresholds, the map in Figure 8 (related to the average values of  
329 the four surveys) shows that many zones (about 49% of the study area) exceeded the threshold  
330 value (TV) set in the Annex III of the Commission staff working document of the GWD  
331 2006/118/EC. In some of these zones (9% of the domain), the predicted values also exceeded the  
332 natural background level (NBL) of 74 µg/L suggested by the “A.Li.Na” project. In particular, in the  
333 central-western region of the area between the Padua and Venice provinces (including Piezometers  
334 9, 10, 20, 37, 40 and 44), the predicted arsenic concentrations were greater than the TV, ranging  
335 from 33.75 to 224 µg/L. Similarly, arsenic concentrations reached the maximum value of 95 µg/L in

336 the eastern region of the study area, near the Venice airport (Piezometer 15). Examining the ORP  
337 overlaid post-map, the ORP values denoted a reducing environment in these areas, in agreement  
338 with the results of several studies on the role of ORP in As release (Carraro et al., 2015, 2013; Dalla  
339 Libera et al., In Press; McArthur et al., 2001; Molinari et al., 2015; Nickson et al., 2000; Rotiroti et  
340 al., 2014). These reducing conditions occur also in some “green” and “yellow” zones but in this  
341 case arsenic is low cause the As-bearing material are missing in the subsoil. Otherwise, analyzing  
342 the available stratigraphic logs (Figure 9), the presence of peat layers is evident in the areas with  
343 high concentrations, confirming the role of organic matter as a redox driver of As release (Dalla  
344 Libera et al., In Press; Molinari et al., 2013; Nickson et al., 2000; Rotiroti and Fumagalli, 2013;  
345 Rotiroti et al., 2014; Ungaro et al., 2008). From a hydrogeological perspective, a map analysis  
346 suggested that the arsenic contamination disagreed with the groundwater natural drainage and did  
347 not spread in accordance with the groundwater flow directions (NW-SE) (Fabbri, 2013).



348

349 **Figure 8.** Original prediction of arsenic concentration within the DBVL. This map shows the raw  
 350 prediction results obtained by the COK method. The contour lines represent the arsenic  
 351 concentration values basing on the COK prediction with an interval of 5  $\mu\text{g/L}$ . The bold lines are  
 352 the main contours.



353

354 **Figure 9.** The reclassified arsenic prediction , obtained from the raw prediction in figure 8, and the  
 355 ORP post-map. The stratigraphic log shows some peat layers corresponding to the zones with high  
 356 arsenic values. The red boxes highlight the peat layers.

357 **5.3.Implications for water and environmental management**

358 Groundwater arsenic pollution in alluvial systems can result from natural processes, such as  
 359 weathering, the interaction between groundwater and mineral deposits or the degradation of organic  
 360 matter deposits (e.g., peat layers). The distinction between anthropogenic and natural sources of  
 361 contamination is important for approaching the contamination issues. Therefore, the evaluation of  
 362 an NBL value plays an important role in highlighting anthropogenic pollution. The methods,  
 363 suggested by the EU BRIDGE project, provide a statistically representative value for the entire  
 364 study area but does not take into consideration the spatial distribution of the data. Our approach  
 365 suggests a Local Natural Background Levels (LNBLs), combining the 90<sup>th</sup> percentile concept and  
 366 the spatial data distribution and defining two or three classes (depending to the difference between  
 367 TV and NBL), in which we can estimate the LNBLs. In this way, the errors between the natural

368 occurrence and the man-made pollution are minimized. By considering a unique NBL value for the  
369 entire area, an incorrect distinction between natural occurrence and pollution could occur. For  
370 example, in zones with a concentration lower than the NBL, we risk accepting an external pollution  
371 as a natural occurrence. However, in an area belonging to a higher class, we risk misinterpreting a  
372 natural occurrence as pollution. Therefore, we suggest calculating a local NBL using only the data  
373 inside the areas, defined by concentration classes established using a geostatistical prediction (e.g.,  
374 the green areas in Figure 6 with predicted values between 0.5 and 10  $\mu\text{g/L}$ ). This step could be  
375 easily conducted if the number of available data is significantly adequate in each class ( $n \geq 30$ )  
376 (Müller et al., 2006). If the number of data is lower than 30, the sampling network should be  
377 enhanced. Referring to the DBVL area, all three identified zones have a number of piezometers  
378 fewer than 30 in the “A.Li.Na” sampling network. Therefore, a significant calculation of the LNBL  
379 was not performed. However, in the green areas (about 51% of the study area, Figure 9) with a  
380 predicted arsenic concentration between 0.5 to 10  $\mu\text{g/L}$  (TV), 24 piezometers are available. For  
381 example, in these areas, the LNBL was estimated to be equal to 6.68  $\mu\text{g/L}$ , according to the  
382 BRIDGE project method. Such a result shows that the LNBL value is not only much lower than the  
383 “A.Li.Na” NBL value (74  $\mu\text{g/L}$ ) but is also lower than the TV (10  $\mu\text{g/L}$ ).

## 384 **6. CONCLUSIONS**

385 The results presented in this paper show how a geostatistical spatial approach allows for the  
386 application of the 90<sup>th</sup> percentile method (NBL) in a more critical way. The map of the natural  
387 distribution of arsenic allows for the identification of critical areas, highlighting where the As  
388 values exceed the TV. In particular, this result illustrates the usefulness of calculating a local NBL  
389 (LNBL) related to the different defined areas. Using the cokriging approach, the definition of  
390 LNBLs takes advantage of the arsenic spatial distribution and the geochemical relationships among  
391 arsenic and other related parameters. In fact, the correlations between arsenic and auxiliary  
392 variables, such as Fe and  $\text{NH}_4^+$ , are taken into consideration for cokriging prediction. The results of

393 this study highlight the critical issues related to the application of a single NBL value at the regional  
394 scale. Through the BRIDGE suggestions, the European GWD proposes a NBL value without  
395 considering the spatial distribution of the parameter concentration or the geochemical relations  
396 among the correlated parameters. The LNBL concept aims to reduce the error associated with the  
397 distinction between the natural occurrence of arsenic and anthropogenic pollution. By defining a  
398 LNBL for every class of concentration, monitoring the anthropogenic pollution events is easy,  
399 particularly for the lower and intermediate classes (see Table 2). In addition, the proposed approach  
400 might be applied to a global view of the study area, informing decisions about water and  
401 environmental management and improving the characterization plan necessary to evaluate  
402 potentially contaminated sites. Finally, the suggested approach is easily applicable to estimate the  
403 LNBL of any kind of elements or compound deriving from natural processes, both in groundwater  
404 and soil.

405 **Author Contributions**

406 The manuscript was written through contributions of all authors. All authors have given approval to  
407 the final version of the manuscript.

408 **Notes**

409 The authors declare no competing financial interest.

410 **ACKNOWLEDGMENT**

411 This work was founded by the Venice Province, project “IDRO”, grant to P. Fabbri. We thank the  
412 ARPAV agency, in particular the internal water observatory, to share their data concerning the  
413 arsenic groundwater contamination into the DBVL.

414 **REFERENCES**

415 APAT, 2003. Analytical methods for chemical water analysis, vol. 1. Handbooks and guidelines,  
416 29, I.G.E.R. srl, Roma.

417 APAT, 2006. Handbook for environmental investigation upon contaminated sites. Handbooks and  
418 guidelines, I.G.E.R. srl, Roma.

419 ARPA, 2014. ALiNa – Analysis of the Natural Background Level for some compounds within the  
420 groundwater of the shallow aquifer in the Drainage Basin to the Venice Lagoon (Brenta river  
421 alluvial system) – Report and data presentation.

422 Baiocchi, A., Lotti, F., Piscopo, V., 2011. Influence of hydrogeological setting on the arsenic  
423 occurrence in groundwater of the volcanic areas of central and southern Italy. *AQUA mundi* 2,  
424 131–142. doi:10.4409/Am-035-11-0035

425 Baviskar, S., Choudhury, R., Mahanta, C., 2015. Dissolved and solid-phase arsenic fate in an  
426 arsenic-enriched aquifer in the river Brahmaputra alluvial plain. *Environ. Monit. Assess.* 187, 93.  
427 doi:10.1007/s10661-015-4277-0

428 Biswas, A., Gustafsson, J.P., Neidhardt, H., Halder, D., Kundu, A.K., Chatterjee, D., Berner, Z.,  
429 Bhattacharya, P., 2014. Role of competing ions in the mobilization of arsenic in groundwater of  
430 Bengal Basin: Insight from surface complexation modeling. *Water Res.* 55, 30–39.  
431 doi:10.1016/j.watres.2014.02.002

432 Bivand R.S., Pebesma E.J., Gomez-Rubio V., 2009. *Applied spatial data analysis with R*; Springer,  
433 ISBN 978-0-387-78170-9, DOI: 10.1007/978-0-387-78171-6

434 Bondesan, A., Meneghel, M., 2004. *Geomorphology of the Venice Province (in Italian)*. Esedra,  
435 Padova.

436 Cambuzzi T., Conchetto E., Fabbri P., Marcolongo E., Rosignoli A., Zangheri P., 2009.  
437 Groundwater resources in the middle Venetian plain. *Rend. Online Soc. Geol. It.*, 6, 127-128.

438 Carraro, A., Fabbri, P., Giaretta, A., Peruzzo, L., Tateo, F., Tellini, F., 2015. Effects of redox  
439 conditions on the control of arsenic mobility in shallow alluvial aquifers on the Venetian Plain  
440 (Italy). *Sci. Total Environ.* 532, 581–594. doi:10.1016/j.scitotenv.2015.06.003

441 Carraro, A., Fabbri, P., Giaretta, A., Peruzzo, L., Tateo, F., Tellini, F., 2013. Arsenic anomalies in  
442 shallow Venetian Plain (Northeast Italy) groundwater. *Environ. Earth Sci.* 70, 3067–3084.  
443 doi:10.1007/s12665-013-2367-2

444 Cleveland W.S., 1979. Robust Locally Weighted Regression and Smoothing Scatterplots. *Journal of*  
445 *the American statistical association*, Vol. 74, No. 368, pp. 829 – 836.

446 Coetsiers, M., Blaser, P., Martens, K., Walraevens, K., 2009. Natural background levels and  
447 threshold values for groundwater in fluvial Pleistocene and Tertiary marine aquifers in Flanders,  
448 Belgium. *Environ. Geol.* 57, 1155–1168. doi:10.1007/s00254-008-1412-z

449 Dalla Libera N., Fabbri P., Mason L., Piccinini L., Pola M., (In press). Natural Arsenic in  
450 groundwater in the drainage basin to the Venice lagoon (Brenta Plain, NE Italy): the organic  
451 matter's role. *Rend. Online Soc. Geol. It.*

452 Dal Prà, A., Fabbri, P., Bortoletto, C., 1992. The artesian hydrogeological system and its  
453 exploitation in the area between the Treviso City and the Piave River (in Italian). *Memorie di*  
454 *Scienze Geologiche*, 44, 151-170.

455 D. Lgs. 152/06, 2006. Legislative Decree on environmental regulations.

456 D. Lgs. 30/09, 2009. Legislative Decree on the implementation of Directive 2006/118/EC on the  
457 protection of groundwater from contamination and degradation.

458 Edmunds, W.M., Shand, P., 2008. *Natural Groundwater Quality*. Wiley-Blackwell (488 pp., ISBN  
459 978-14051- 5675-2).

460 Fabbri, P., Piccinini, L., Marcolongo, E., Pola, M., Conchetto, E., Zangheri, P., 2016. Does a  
461 change of irrigation technique impact on groundwater resources? A case study in Northeastern Italy.  
462 *Environ. Sci & Policy*. 63, 63.75. doi: 10.1016/j.envsci.2016.05.009

463 Fabbri, P., Gaetan, C., Zangheri, P., 2011. Transfer function-noise modelling of an aquifer system  
464 in NE Italy. *Hydrol. Process*. 25, 194–206. doi:10.1002/hyp.7832

465 Fabbri, P., Piccinini, L., 2013. Assessing transmissivity from specific capacity in an alluvial aquifer  
466 in the middle Venetian plain (NE Italy). *Water Sci. Technol.* 67, 2000–2008.  
467 doi:10.2166/wst.2013.074

468 Fabbri, P., Zangheri, P., Bassan, V., Fagarazzi, E., Mazzucato, A., Primon, S., Zogno, C., 2013.  
469 *Hydrogeology of the Venice Province – The shallow aquifers* (in Italian). Venice Province –  
470 University of Padova.

471 Fendorf, S., Michael, H.A., van Geen, A., 2010. Spatial and Temporal Variations of Groundwater  
472 Arsenic in South and Southeast Asia. *Science* (80-. ). 328, 1123–1127.  
473 doi:10.1126/science.1172974

474 Fontana, A., Mozzi, P., Bondesan, A., 2004. The geomorphological evolution of the Venetian-  
475 Friulian plain (in Italian). *Whitin the: Bondesan, A., Meneghel, M., 2004. Geomorphology of the*  
476 *Venice Province. Esedra, Padova. 113-138.*

477 Fontana, A., Mozzi, P., Bondesan, A., 2008. Alluvial megafans in the Venetian–Friulian Plain  
478 (northeastern Italy): Evidence of sedimentary and erosive phases during Late Pleistocene and  
479 Holocene. *Quaternary International*, 189, 71-90.

480 GWD, 2006. Groundwater Directive 2006/118/CE, Directive of the European Parliament and of the  
481 Council on the protection of groundwater against pollution and deterioration, OJ L372, 27/12/ 2006,  
482 pp 19–31.

483 Hinsby, K., Condesso de Melo, M.T., Dahl, M., 2008. European case studies supporting the  
484 derivation of natural background levels and groundwater threshold values for the protection of  
485 dependent ecosystems and human health☆. *Sci. Total Environ.* 401, 1–20.  
486 doi:10.1016/j.scitotenv.2008.03.018

487 Isaaks E.H., Srivastava R.M. *An introduction to Applied Geostatistics*; Oxford University Press:  
488 New York, 1989.

489 McArthur, J.M., Banerjee, D.M., Hudson-Edwards, K.A., Mishra, R., Purohit, R., Ravenscroft, P.,  
490 Cronin, A., Howarth, R.J., Chatterjee, A., Talukder, T., Lowry, D., Houghton, S., Chadha, D.K.,  
491 2004. Natural organic matter in sedimentary basins and its relation to arsenic in anoxic ground  
492 water: The example of West Bengal and its worldwide implications. *Appl. Geochemistry* 19, 1255–  
493 1293. doi:10.1016/j.apgeochem.2004.02.001

494 McArthur, J.M., Ghosal, U., Sikdar, P.K., Ball, J.D., 2016. Arsenic in Groundwater: The Deep Late  
495 Pleistocene Aquifers of the Western Bengal Basin. *Environ. Sci. Technol.* 50, 3469–3476.  
496 doi:10.1021/acs.est.5b02477

497 McArthur, J.M., Ravenscroft, P., Safiulla, S., Thirlwall, M.F., 2001. Arsenic in groundwater:  
498 Testing pollution mechanisms for sedimentary aquifers in Bangladesh. *Water Resour. Res.* 37, 109–  
499 117. doi:10.1029/2000WR900270

500 Molinari, A., Guadagnini, L., Marcaccio, M., Guadagnini, A., 2015. Arsenic fractioning in natural  
501 solid matrices sampled in a deep groundwater body. *Geoderma* 247-248, 88–96.  
502 doi:10.1016/j.geoderma.2015.02.011

503 Molinari, A., Guadagnini, L., Marcaccio, M., Guadagnini, A., 2012. Natural background levels and  
504 threshold values of chemical species in three large-scale groundwater bodies in Northern Italy. *Sci.*  
505 *Total Environ.* 425, 9–19. doi: 10.1016/j.scitotenv.2012.03.015

506 Molinari, A., Guadagnini, L., Marcaccio, M., Straface, S., Sanchez-Vila, X., Guadagnini, A., 2013.  
507 Arsenic release from deep natural solid matrices under experimentally controlled redox conditions.  
508 *Sci. Total Environ.* 444, 231–240. doi: 10.1016/j.scitotenv.2012.11.093

509 Mozzi P., Bini C., Zilocchi L., Beccatini R., Mariotti Lippi M., 2003. Stratigraphy, palaeopedology  
510 and palynology of late Pleistocene and Holocene deposits in the landward sector of the lagoon of  
511 Venice (Italy), in relation to Caranto level. *Il Quaternario*, 16 (1 bis), pag. 193 – 210.

512 Müller D., Blum A., Hart A., Hookey J., Kunkel R., Scheidleder A., Tomlin C., Wendland F., 2006.  
513 BRIDGE Project: Background criteria for identification of groundwater thresholds, D18: Final  
514 proposal for a methodology to set up groundwater threshold values in Europe.

515 Nickson, R., McArthur, J., Burgess, W., Ahmed, K.M., Ravenscroft, P., Rahman, M., 1998. Arsenic  
516 poisoning of Bangladesh groundwater. *Nature* 395, 338. doi:10.1038/26387

517 Nickson, R.T., Mearthur, J.M., Ravenscroft, P., Burgess, W.G., Ahmed, K.M., 2000. Mechanism of  
518 arsenic release to groundwater, Bangladesh and West Bengal. *Appl. Geochemistry* 15, 403–413.  
519 doi:10.1016/S0883-2927(99)00086-4

520 Nordstrom, D.K., 2003. *Arsenic in Ground Water*, Science Mag. Springer US, Boston, MA.  
521 doi:10.1007/b101867

522 Pebesma, E.J., 2004. Multivariable geostatistics in S: the gstat package. *Comput. Geosci.* 30, 683–  
523 691. doi: 10.1016/j.cageo.2004.03.012

524 Piccinini, L., Fabbri, P., Pola, M., 2016. Point dilution tests to calculate groundwater velocity, an  
525 example in a porous aquifer in NE Italy. *Hydrol. Sci. J.* 61(8), 1512-1523.  
526 doi:10.1080/02626667.2015.1036756

527 Piccinini, L., Fabbri, P., Pola, M., Marcolongo, E., Rosignoli, A., 2015. Numerical modeling to  
528 well-head protection area delineation, an example in Veneto Region (NE Italy). *Rend. Online Soc.*  
529 *Geol. It.* 35, 232-235. doi: 10.3301/ROL.2015.108

530 Preziosi, E., Giuliano, G., Vivona, R., 2010. Natural background levels and threshold values  
531 derivation for naturally As, V and F rich groundwater bodies: a methodological case study in  
532 Central Italy. *Environ. Earth Sci.* 61, 885–897. doi:10.1007/s12665-009-0404-y

533 Posa D., De Iaco S., 2009. *Geostatistics, theory and applications*. G. Giappichelli Editore, Turin,  
534 Italy, ISBN 978-88-348-9744-7

535 R Core Team, 2015. *R: A language and environment for statistical computing*, R Foundation for  
536 Statistical Computing, Vienna, Austria. URL: <http://www.R-project.org/>

537 Rango, T., Vengosh, A., Dwyer, G., Bianchini, G., 2013. Mobilization of arsenic and other  
538 naturally occurring contaminants in groundwater of the main ethiopian rift aquifers. *Water Res.* 47,  
539 5801–5818. doi:10.1016/j.watres.2013.07.002

540 Rotiroti, M., Fumagalli, L., 2013. Derivation of preliminary natural background levels for naturally  
541 Mn, Fe, As and NH<sub>4</sub><sup>+</sup> rich groundwater: The case study of Cremona area (Northern Italy). *Rend.*  
542 *Online Soc. Geol. Ital.* 24, 284–286.

543 Rotiroti, M., Sacchi, E., Fumagalli, L., Bonomi, T., 2014. Origin of Arsenic in Groundwater from  
544 the Multilayer Aquifer in Cremona (Northern Italy). *Environ. Sci. Technol.* 48, 5395–5403.  
545 doi:10.1021/es405805v

546 Rowland, H.A.L., Pederick, R.L., Polya, D.A., Pancost, R.D., Van Dongen, B.E., Gault, A.G.,  
547 Vaughan, D.J., Bryant, C., Anderson, B., Lloyd, J.R., 2007. The control of organic matter on  
548 microbially mediated iron reduction and arsenic release in shallow alluvial aquifers, Cambodia.  
549 *Geobiology* 5, 281–292. doi:10.1111/j.1472-4669.2007.00100.x

550 Smedley, P.L., Kinniburgh, D.G., 2002. A review of the source, behaviour and distribution of  
551 arsenic in natural waters. *Appl. Geochemistry* 17, 517–568. doi:10.1016/S0883-2927(02)00018-5

552 Sorg, T.J., Chen, A.S.C., Wang, L., 2014. Arsenic species in drinking water wells in the USA with  
553 high arsenic concentrations. *Water Res.* 48, 156–169. doi:10.1016/j.watres.2013.09.016

554 Takeno, N., 2005. Atlas of Eh-pH diagrams Intercomparison of thermodynamic databases. *Natl.*  
555 *Inst. Adv. Ind. Sci. Technol.* Tokyo 285.

556 Trevisani, S., Fabbri, P., 2010. Geostatistical modeling of a heterogeneous site bordering the Venice  
557 lagoon, Italy. *Ground Water* 48, 614–623. doi:10.1111/j.1745-6584.2009.00632.x

558 Ungaro, F., Ragazzi, F., Cappellin, R., Giandon, P., 2008. Arsenic concentration in the soils of the  
559 Brenta Plain (Northern Italy): Mapping the probability of exceeding contamination thresholds. *J.*  
560 *Geochemical Explor.* 96, 117–131. doi:10.1016/j.gexplo.2007.03.006

561 Vorlicek, P.A., Antonelli, R., Fabbri, P., Rausch, R., 2004. Quantitative hydrogeological studies of  
562 the Treviso alluvial plain, NE Italy. *Q. J. Eng. Geol. Hydrogeol.* 37, 23–29. doi:10.1144/0036-  
563 9276/02-006

564 Welch, A.H., Westjohn, D.B., Helsel, D.R., Wanty, R.B., 2000. Arsenic in Ground Water of the  
565 United States: Occurrence and Geochemistry. *Ground Water* 38, 589–604. doi:10.1111/j.1745-  
566 6584.2000.tb00251.x

567 Wendland, F., Berthold, G., Blum, A., Elsass, P., Fritsche, J.-G., Kunkel, R., Wolter, R., 2008a.  
568 Derivation of natural background levels and threshold values for groundwater bodies in the Upper  
569 Rhine Valley (France, Switzerland and Germany). *Desalination* 226, 160–168.  
570 doi:10.1016/j.desal.2007.01.240

571 Wendland, F., Blum, A., Coetsiers, M., Gorova, R., Griffioen, J., Grima, J., Hinsby, K., Kunkel, R.,  
572 Marandi, A., Melo, T., Panagopoulos, A., Pauwels, H., Ruisi, M., Traversa, P., Vermooten, J.S.A.,  
573 Walraevens, K., 2008b. European aquifer typology: A practical framework for an overview of  
574 major groundwater composition at European scale. *Environ. Geol.* 55, 77–85. doi:10.1007/s00254-  
575 007-0966-5

576 Zavatti, A.; Attramini, D.; Bonazzi, A.; Boraldi, V.; Malagò, R.; Martinelli, G.; Naldi, S.; Patrizi,  
577 G.; Pezzera, G.; Vandini, W.; Venturini, L.; Zuppi, G. M., 1995. Occurrence of groundwater arsenic  
578 in the Po Plain: Environmental evidences and geochemical hypothesis. *Quad. Geol. Appl.*, S2,  
579 2.301–2.326.